

An Improved DCT-Based Image Watermarking Scheme Using Fast Walsh Hadamard Transform

Aris Marjuni, Mohammad Faizal Ahmad Fauzi, Rajasvaran Logeswaran, and Swee-Huay Heng

Abstract—Image watermarking is of interesting in the multimedia and information security research fields. This paper presents an improved discrete cosine transform (DCT)-based image watermarking scheme using the fast Walsh Hadamard transform (FWHT) for image authentication. As a fast transformation with good energy compaction, this transform is frequently applied in image processing operations, such as image data compression and filtering. In the proposed scheme, the fast Walsh Hadamard transform is applied to the watermark signal before it is embedded into the DCT coefficients. The low signal coefficients are expected to produce a high visual quality of the watermarked image. The performance of the proposed scheme is then compared with the DCT-based image watermarking scheme performance itself. This experiment is simulated by several attacks to test the robustness of the watermark, such as noise insertion, JPEG compression, cropping, rotation, and scaling. Experimental results show that the imperceptibility of the watermarked image could be improved. The robustness of the watermark is also improved depend on the level distortion.

Index Terms—Image watermarking, discrete cosine transform, fast Walsh Hadamard transform, imperceptibility, robustness, watermarked image.

I. INTRODUCTION

Digital images have increasingly significant roles in the information technology age. They are used in many application areas, such as in business, communication, entertainment, education, information security, authentication, intellectual property protection, broadcast monitoring, fingerprinting, copyright management, tamper detection, etc., where much of the information can be received, stored and presented visually in the form of images. As a digital content, an image can be produced, stored, distributed, and manipulated easily. However, it is very susceptible to being copied by unauthorized persons and difficult to distinguish copies from the original. Image watermarking can be used in such situations for image authentication, in this case, these digital contents will be protected by watermark [1]-[3]. Generally, the image watermarking technique protects the host image with data or information, which is embedded permanently in the host image using the watermark

embedding scheme. The watermark should be detected and/or extracted from the watermarked image using the watermark extraction scheme. Thus, an image watermarking technique consists of two processes [4], namely watermark embedding and watermark extraction.

Image watermarking has to satisfy two main properties: imperceptibility and robustness. Imperceptibility describes the visual quality of the watermarked image. Robustness reflects the resilience of the watermark from many kinds of attacks, meaning that the watermark could be extracted or recovered even if the watermarked image is altered. Those properties are important requirements for a good watermark, but it is difficult to achieve high levels of both at the same time. Hence, many new image watermarking schemes were proposed to improve the quality of watermarks [1], [3]-[5].

There are two main approaches in image watermarking, which are spatial domain and frequency domain. The least significant bits (LSB) technique is frequently used in the spatial domain, whereas, the discrete cosine transform (DCT), discrete Fourier transform (DFT) and discrete wavelet transform (DWT), are the most popular techniques in the frequency domain. Many new schemes have been developed to improve the watermark requirements in both domains, such as between DWT and DCT [6].

In order to use the Hadamard transform in digital watermarking scheme, several methods have been proposed. In [7], the multi resolution Walsh Hadamard transform using singular value decomposition (SVD) was proposed to improve both imperceptibility and robustness. First, the host image is transformed by multi resolution Walsh Hadamard transform, and then the watermark was embedded in the middle singular values of the high frequency sub-bands at the coarsest and the finest level. In [8], the watermarks were embedded into Hadamard transform coefficients which are controlled by pseudo-radon permutation as a security key, while extraction process is implemented without the host image. In [9], the original image is decomposed into 4x4 blocks, and then a gray-level watermark was embedded into the estimated values of two first AC coefficients of Hadamard transform.

The different approaches on the watermarking scheme were also proposed in [10], [11]. In [10], the complex Hadamard transform is used to propose the watermarking scheme for still digital image based on the sequency-ordered. The proposed method in [11] also used the complex Hadamard transform, where the watermark was embedded in the imaginary part of the transform coefficients. The other method has been proposed using Hadamard transform to obtain a perceptually adaptive spread transform image watermarking, as in [12].

Manuscript received October 30, 2012; revised December 14, 2012.

Aris Marjuni and Mohammad Faizal Ahmad Fauzi are with the Faculty of Engineering, Multimedia University, Cyberjaya 63100, Selangor, Malaysia (e-mail: arism240669@gmail.com, faizal1.mmu@mmu.edu.my).

Rajasvaran Logeswaran is with the School of Engineering, Science and Technology, Nilai University College 71800 Nilai, Negeri Sembilan, Malaysia (e-mail: logeswaran@gmail.com).

Swee-Huay Heng is with the Faculty of Information Science & Technology, Multimedia University, Bukit Beruang 75450, Melaka, Malaysia (e-mail: shheng@mmu.edu.my).

In this paper, we present the FWHT combined with DCT (FWHT-DCT) as a new approach in the digital image watermarking scheme based on Hadamard transform. The FWHT is applied on the original watermark before it is embedded into the DC coefficients of the host image. The motivation to apply this transform is that it offers several advantages, such as higher image fidelity [12]. The initial experiment using FWHT-DCT has been performed, as in [13].

The further experiments and analysis is performed in this paper as an improvement of the initial project, which is organized as follows. Section II presents the DCT based image watermarking scheme. The proposed FWHT-DCT image watermarking scheme is described in Section III. Section IV provides the measures used to analyze the watermark performance. Section V describes the experimental results and performance analysis of the proposed scheme compared with the common DCT scheme. Finally, the conclusion is presented in Section VI.

II. DCT BASED IMAGE WATERMARKING

A. Discrete Cosine Transform (DCT)

The Discrete Cosine Transform (DCT) is a well-known image transformation which is used in many image processing applications. This transform attempts to de-correlate the image data, allowing each transform coefficient to be encoded independently without losing compression efficiency. The one-dimensional discrete cosine transform (1D-DCT) is defined in (1), as in [4].

$$C(u) = \alpha(u) \sum_{x=0}^{N-1} f(x) \cos\left(\frac{\pi(2x+1)u}{2N}\right) \quad (1)$$

$$u = 0, 1, 2, \dots, N-1$$

The inverse of one-dimensional discrete cosine transform (i1D-DCT) is defined as:

$$f(x) = \alpha(u) \sum_{u=0}^{N-1} C(u) \cos\left(\frac{\pi(2x+1)u}{2N}\right) \quad (2)$$

$$x = 0, 1, 2, \dots, N-1$$

$\alpha(u)$ is defined as:

$$\alpha(u) = \begin{cases} \frac{1}{\sqrt{N}}, & \text{if } u=0 \\ \frac{\sqrt{2}}{\sqrt{N}}, & \text{otherwise} \end{cases} \quad (3)$$

$$C(u=0) = \frac{1}{\sqrt{N}} \sum_{x=0}^{N-1} f(x) \quad (4)$$

for $u = 0$

And the first transform coefficient is the average value of the sample sequence. This value is referred to as the DC coefficient, and all other transform coefficients are called the AC coefficients. The two-dimensional DCT (2D-DCT) is a

direct extension of the 1D-DCT case [4] and is given by:

$$C(u, v) = \alpha(u)\alpha(v) \sum_{x=0}^{N-1} \sum_{y=0}^{N-1} f(x, y) \cos\left(\frac{\pi(2x+1)u}{2N}\right) \cos\left(\frac{\pi(2y+1)v}{2N}\right) \quad (5)$$

$$u, v = 0, 1, 2, \dots, N-1$$

The inverse transform (i2D-DCT) is defined as:

$$f(x, y) = \alpha(u)\alpha(v) \sum_{u=0}^{N-1} \sum_{v=0}^{N-1} C(u, v) \cos\left(\frac{\pi(2x+1)u}{2N}\right) \cos\left(\frac{\pi(2y+1)v}{2N}\right) \quad (6)$$

$$x, y = 0, 1, 2, \dots, N-1$$

B. DCT-Based Image Watermarking

In the watermarking scheme based on the DCT, the watermark bits are embedded in each $N \times N$ DCT block of the host image. Take the watermark W of size $N \times N$ and the original image A of size $M \times M$. Apply the DCT to each 8×8 block of the original image A to obtain the DC coefficients B . Before the watermark is embedded, generate the two pseudorandom number (PN) sequences k_1 and k_2 using the same seed. Then, embed the PN sequences with gain factor α in the DC coefficients B , as shown in (7).

$$B' = \begin{cases} B + \alpha \times k_1, & \text{if } W = 1 \\ B + \alpha \times k_2, & \text{otherwise} \end{cases} \quad (7)$$

Finally, apply the inverse of DCT (IDCT) on DC component B' to reconstruct the watermarked image A' [4].

The watermark extraction is performed by applying the DCT to each 8×8 block of the watermarked image. After the DC coefficients are obtained, calculate the correlation coefficient between the DC coefficients X' and the two PN sequences k_1 and k_2 to each 8×8 block of watermarked image, i.e. $c(B', k_1)$, and $c(B', k_2)$. The watermark is extracted by comparing those correlation coefficients by (8).

$$W' = \begin{cases} 1, & \text{if } c(B', k_1) < c(B', k_2) \\ 0, & \text{otherwise} \end{cases} \quad (8)$$

III. PROPOSED FWHT-DCT BASED IMAGE WATERMARKING

A. Fast Walsh Hadamard (FWH) Transform

The Hadamard transform matrix is an orthogonal square matrix which only has 1 and -1 element values. This transform is also known as Walsh-Hadamard transform. H_1 is the smallest Hadamard matrix [9], [13]-[17] and it is defined as:

$$H_1 = \frac{1}{\sqrt{2}} \begin{bmatrix} 1 & 1 \\ 1 & -1 \end{bmatrix} \quad (9)$$

$$H_N = H_1 \otimes H_{N-1} = \begin{bmatrix} H_{N-1} & H_{N-1} \\ H_{N-1} & -H_{N-1} \end{bmatrix} \quad (10)$$

The Hadamard matrix H_N of size N is constructed by the Kronecker product between H_1 and H_{N-1} , where $N=2^n$, n is an

integer number. Eq. (11) shows an example of a 4×4 Hadamard matrix, which H_2 is obtained using (9) and (10).

$$H_2 = H_1 \otimes H_1 = \frac{1}{2} \begin{bmatrix} 1 & 1 & 1 & 1 \\ 1 & -1 & 1 & -1 \\ 1 & 1 & -1 & -1 \\ 1 & -1 & -1 & 1 \end{bmatrix} \begin{matrix} \text{Sign Changes} \\ 0 \\ 3 \\ 1 \\ 2 \end{matrix} \quad (11)$$

The number of sign changes along each row of the matrix in (11) is called the sequency of the row. These rows can be considered to be samples of rectangular waves with a sub period of $1/N$ units. These continuous functions are called Walsh's functions [15]. The normalized Hadamard matrix is an orthogonal matrix and satisfies the following relation:

$$H_h \times H_h^T = I \quad (12)$$

The H_h is the Hadamard matrix, H_h^T is the inverse Hadamard matrix, and I is the unitary matrix. The Hadamard transform can be computed in $n = \log_2 N$ operations, using the Fast Walsh Hadamard transform. Suppose x is a signal vector, X is a spectrum vector, and H_h is the Hadamard matrix. The forward Walsh Hadamard Transform (WHT) and inverse WHT (IWHT) [17] are defined as:

$$WHT(x) = X = H_w x \quad (13)$$

$$IWHT(X) = x = H_w X \quad (14)$$

The WHT and IWHT is the forward and inverse of WHT_h , respectively, and H_w is the Walsh ordered matrix. The Walsh ordered matrix H_w can be obtained by reordered the rows of the Hadamard matrix H_h , while the Hadamard ordered can be obtained by converting the binary form to gray scale code, as shown in Table I.

TABLE I: SEQUENCY ORDER TO HADAMARD ORDER

Type	Code			
Sequency order	0	1	2	3
Binary	00	01	10	11
Gray code	00	01	11	10
Bit reverse	00	10	11	01
Hadamard order	0	2	3	1

As an example, consider $x = [0, 2, 4, 6]$ a signal vector of $N=4$ elements ($n=2$). The Hadamard and Walsh matrix of this vector are given in (15), respectively.

$$H_h = \frac{1}{2} \begin{bmatrix} 1 & 1 & 1 & 1 \\ 1 & -1 & 1 & -1 \\ 1 & 1 & -1 & -1 \\ 1 & -1 & -1 & 1 \end{bmatrix} \begin{matrix} \text{Sign Changes} \\ 0 \\ 3 \\ 1 \\ 2 \end{matrix} ; \quad (15)$$

$$H_w = \frac{1}{2} \begin{bmatrix} 1 & 1 & 1 & 1 \\ 1 & 1 & -1 & -1 \\ 1 & -1 & -1 & 1 \\ 1 & -1 & 1 & -1 \end{bmatrix} \begin{matrix} \text{Sign Changes} \\ 0 \\ 1 \\ 2 \\ 3 \end{matrix} \quad (16)$$

Furthermore, the forward transform of x can be found as:

$$X = H_w x = \frac{1}{2} \begin{bmatrix} 1 & 1 & 1 & 1 \\ 1 & 1 & -1 & -1 \\ 1 & -1 & -1 & 1 \\ 1 & -1 & 1 & -1 \end{bmatrix} \begin{bmatrix} 0 \\ 2 \\ 4 \\ 6 \end{bmatrix} = \begin{bmatrix} 6 \\ -4 \\ 0 \\ -2 \end{bmatrix} \quad (17)$$

$$x = H_w X = \frac{1}{2} \begin{bmatrix} 1 & 1 & 1 & 1 \\ 1 & 1 & -1 & -1 \\ 1 & -1 & -1 & 1 \\ 1 & -1 & 1 & -1 \end{bmatrix} \begin{bmatrix} 6 \\ -4 \\ 0 \\ -2 \end{bmatrix} = \begin{bmatrix} 0 \\ 2 \\ 4 \\ 6 \end{bmatrix} \quad (18)$$

Finally, we have $FHWT(x) = [0, 2, 4, 6]$ as a FWH transform of x and $IFWHT(X) = [0, 2, 4, 6] = x$ as an inverse.

The forward and inverse WHT can also defined as a linear combination of a set of square waves of different sequencies. Those formulas are given in (19) and (20), respectively.

$$X_w(k) = \sum_{n=0}^{N-1} x(n)w_N(k, n) \quad (19)$$

$$= \sum_{n=0}^{N-1} x(n) \prod_{i=0}^{M-1} (-1)^{n_i k_{M-i}}, k = 0, 1, \dots, N-1$$

$$x(n) = \frac{1}{N} \sum_{k=0}^{N-1} X_w(k)w_N(k, n) \quad (20)$$

$$= \frac{1}{N} \sum_{k=0}^{N-1} X_w(k) \prod_{i=0}^{M-1} (-1)^{n_i k_{M-i}}, n = 0, 1, \dots, N-1$$

where $N=2^n$, $M=\log_2 N$, and n_i is the i -th bit in the binary representation of n .

For an example, consider $x = [0, 2, 4, 6]$ as a signal vector with $N=4$ (or $n=2$). Using Table I, (19) and (20), the forward WHT of x can be obtained as follows:

$$X_w(0) = (0).(1) + (2).(1) + (4).(1) + (6).(1) = 12;$$

$$X_w(1) = (0).(1) + (2).(1) + (4).(-1) + (6).(-1) = -8;$$

$$X_w(2) = (0).(1) + (2).(-1) + (4).(-1) + (6).(1) = 0;$$

$$X_w(3) = (0).(1) + (2).(-1) + (4).(1) + (6).(-1) = -4;$$

and, $X=1/2 [12, -8, 0, -4] = [6, -4, 0, -2]$. This result has the same with the values in (17). And the inverse WHT of X is obtained as follows:

$$x(0) = (6).(1) + (-4).(1) + (0).(1) + (-2).(1) = 0;$$

$$x(1) = (6).(1) + (-4).(1) + (0).(-1) + (-2).(-1) = 4;$$

$$x(2) = (6).(1) + (-4).(-1) + (0).(-1) + (-2).(1) = 8;$$

$$x(3) = (6).(1) + (-4).(-1) + (0).(1) + (-1).(-2) = 12;$$

Thus, $x=1/2 [0, 4, 8, 12] = [0, 2, 4, 6]$. The computation of FWH algorithm can be illustrated in Fig. 1 [17].

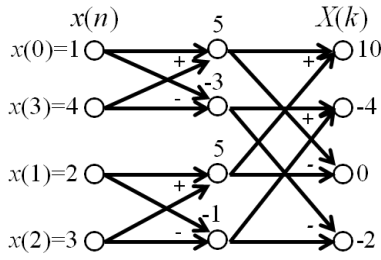


Fig. 1. Computation of FWHT algorithm.

B. FWHT-DCT Based Image Watermarking

The FWHT-DCT based image watermarking is performed by applying the FWHT of the watermark before it is embedded into the host image using DCT. Similar to the DCT scheme, the DCT is applied to each 8×8 block of the original image A to obtain the DC coefficients B . The FWHT of B is then performed in each block, i.e. B' .

Let μ and σ be the mean and standard deviation of the DC vector, respectively, and ρ be the ratio of mean and standard deviation of the DC vector. The inverse FWHT of the two pseudorandom number (PN) sequences k_1 and k_2 , i.e. k_1' and k_2' are used to embed the watermark in the DC coefficient B' using (21).

$$B_w = \begin{cases} B' + \alpha \times (\sqrt{NT_1}k_1'), & \text{if } W = 0 \\ B' + \alpha \times (\sqrt{NT_2}k_2'), & \text{otherwise} \end{cases} \quad (21)$$

where W is the watermark of size $N \times N$ ($N=2^m$; $m=1, 2, \dots$), $T_1 = \rho$ and $T_2 = (1-\rho)$. The coefficient T_1 and T_2 are used to improve the visual quality of the watermarked image. To reconstruct the watermarked image A' , apply the IDCT and IFWHT on the modified DC component B_w . The brief of proposed watermark embedding is described as follows:

Step 1. Decompose the host image into 8×8 -block and apply the DCT to obtain the DC coefficients B of each block.

Step 2. Apply the FWHT to each 8×8 -block to get the B' .

Step 3. Calculate the parameter μ and σ be as the mean and standard deviation of the DC vector, respectively, and ρ be the ratio of mean and standard deviation of the DC vector.

Step 4. Generate two pseudorandom number sequences k_1 and k_2 , k_1' and k_2' .

Step 5. Embed the watermark using formula in (21).

Step 6. Reconstruct the watermarked image.

For watermark extraction, obtain the DC coefficients for each 8×8 block of the watermarked image. Let q be the inverse FWHT of DC vectors, and then calculate the correlation coefficients between the q , k_1' and k_2' for each 8×8 block of the watermarked image, i.e. $c(q, k_1')$, $c(q, k_2')$ and $c(k_1', k_2')$. The recovered watermark is extracted by comparing those correlation coefficients using the threshold $T = \sqrt{N} \times \beta \times (T_1 T_2)$, where β is the weighted value of ρ . The recovered watermark W' is then compared with the original watermark W to obtain the similarity. The watermark extraction process is shown as follows:

Step 1. Obtain the DC coefficients for each 8×8 -block of the watermarked image.

Step 2. Calculate and compare the correlation coefficient between the q , k_1' and k_2' for each 8×8 block of the

watermarked image, i.e. $c(q, k_1')$, $c(q, k_2')$ and $c(k_1', k_2')$ to construct the recovered watermark.

Step 3. Evaluate the similarity between the recovered watermark and original watermark.

IV. PERFORMANCE MEASUREMENTS

A. Imperceptibility

Imperceptibility is related to the visual quality of the watermarked image caused by embedding the watermark. In this work, we use the Peak Signal to Noise Ratio (PSNR) measure to analyze the imperceptibility of both the DCT and FWHT-DCT based image watermarking schemes. A high PSNR values signifies that the watermarked image is closer the original image. Hence, the watermark is less perceptible (i.e. PSNR of 100% indicates completely imperceptible watermark).

Let A be the original image, A' be the watermarked image, R be the maximum fluctuation in the input image data type, and M be the number of rows or columns in the input image. The PSNR between A and A' is given by (22) [5].

$$PSNR = 10 \times \log_{10} \left(R^2 / \sum_{i=1}^M \sum_{j=1}^N [A(i, j) - A'(i, j)]^2 \right) \quad (22)$$

$$i = 1, 2, \dots, M; j = 1, 2, \dots, N$$

B. Robustness

Robustness measures the watermark's resilience to corruption when extracted from the watermarked image, even after the watermarked image has been distorted or damaged. In this work, the Normalized Cross Correlation (NCC) measure is used to analyze the robustness of both the DCT and FWHT-DCT based image watermarking schemes. The NCC indicates the similarity between the extracted and the original watermarks. An extracted watermark with a high NCC value has high similarity with the original watermark. The range of NCC is between 0 and 1.

The NCC is obtained by calculating the correlation between the original watermark and the recovered watermark [4]. Let W be the original watermark, W' is the recovered watermark, and N is the number of rows or columns in the input images. The NCC between the W and W' is given by (23).

$$NCC = \frac{\sum_{i=1}^M \sum_{j=1}^N [W(i, j) \times W'(i, j)]}{\sum_{i=1}^M \sum_{j=1}^N [W(i, j)]^2} \quad (23)$$

$$i = 1, 2, \dots, M; j = 1, 2, \dots, N$$

V. EXPERIMENTAL RESULTS

In this experiment, we use the standard 'Lena', 'Boat', and 'Pepper' 512×512 gray scale images as the host images, while the original watermark is the 'Stamp' 64×64 gray scale image. These are shown in Fig. 2.

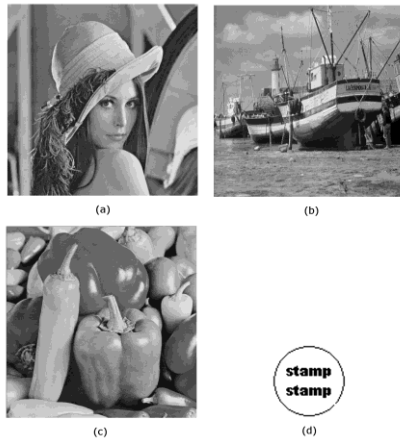


Fig. 2. Host image (a) Lena, (b) Boat, (c) Pepper, and watermark image (d) Stamp.

A. Imperceptibility and Robustness without Attack

The first experiment on both the DCT and FWHT-DCT schemes is for the normal watermarking without any attacks on the watermarked image. The watermarked image and the recovered watermark are shown in Fig. 3. Using the FWHT of the PN sequences allows expansion of the 0 bit where the watermark would be embedded. If w_i is an 8x8 block of the watermark W then w_i' (the FWHT of w_i) would have more 0 bits, as shown in (24).

$$w_i = \begin{bmatrix} 1 & 1 & 1 & 1 & 1 & 1 & 1 & 1 \\ 1 & 1 & 1 & 1 & 1 & 1 & 1 & 1 \\ 1 & 1 & 1 & 1 & 1 & 1 & 1 & 1 \\ 1 & 1 & 1 & 1 & 1 & 1 & 1 & 1 \\ 1 & 1 & 1 & 1 & 1 & 1 & 1 & 1 \\ 1 & 1 & 1 & 1 & 1 & 1 & 1 & 1 \\ 1 & 1 & 1 & 1 & 1 & 1 & 1 & 1 \\ 1 & 1 & 1 & 1 & 1 & 1 & 1 & 1 \end{bmatrix}; w_i' = \begin{bmatrix} 1 & 1 & 1 & 1 & 1 & 1 & 1 & 1 \\ 0 & 0 & 0 & 0 & 0 & 0 & 0 & 0 \\ 0 & 0 & 0 & 0 & 0 & 0 & 0 & 0 \\ 0 & 0 & 0 & 0 & 0 & 0 & 0 & 0 \\ 0 & 0 & 0 & 0 & 0 & 0 & 0 & 0 \\ 0 & 0 & 0 & 0 & 0 & 0 & 0 & 0 \\ 0 & 0 & 0 & 0 & 0 & 0 & 0 & 0 \\ 0 & 0 & 0 & 0 & 0 & 0 & 0 & 0 \end{bmatrix} \quad (24)$$

Larger modifications of the watermark affect its strength. Watermark recovery is performed by analyzing the magnitude difference of the modification of the bit values using the inverse of w_i' , as shown in (25).

$$IFWHT(w_i') = w_i = \begin{bmatrix} 1 & 1 & 1 & 1 & 1 & 1 & 1 & 1 \\ 1 & 1 & 1 & 1 & 1 & 1 & 1 & 1 \\ 1 & 1 & 1 & 1 & 1 & 1 & 1 & 1 \\ 1 & 1 & 1 & 1 & 1 & 1 & 1 & 1 \\ 1 & 1 & 1 & 1 & 1 & 1 & 1 & 1 \\ 1 & 1 & 1 & 1 & 1 & 1 & 1 & 1 \\ 1 & 1 & 1 & 1 & 1 & 1 & 1 & 1 \\ 1 & 1 & 1 & 1 & 1 & 1 & 1 & 1 \end{bmatrix} \quad (25)$$

Using the PSNR values of those images, it appears that the imperceptibility of the watermarked image based on the proposed scheme is increased compared with the DCT scheme. The robustness of the recovered watermarks is slightly decreased because the capacity of the watermark is slightly reduced. However, all of the recovered watermarks are clearly recognizable, as shown in Fig. 3.

B. Imperceptibility and Robustness after Attacks

Experiments using image processing techniques as attacks on the watermarked image were also undertaken. These

include noise insertion, JPEG compression, cropping, rotation and resizing. In each attack, the performance of the watermark between the DCT scheme and FWHT-DCT scheme is compared.

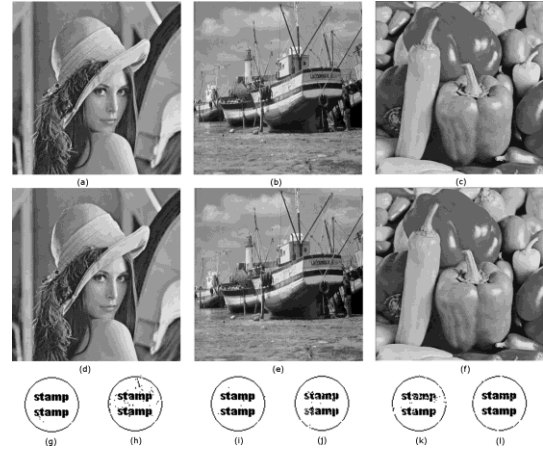


Fig. 3. Watermarked image and recovered watermark without attack; (a) Lena, (b) Boat, (c) Pepper.

1) Noise Insertion Attack

This experiment is performed by adding multiplicative random noise into the watermarked image using the following formula.

$$A'' = A' + d \times p \quad (27)$$

where A'' is the watermarked image influenced by noise, A' is the watermarked image, d is the noise density and p is the pseudorandom integer number.

Depending on the noise density, the insertions have an impact on the imperceptibility level of the watermarked image and the robustness level of the watermark. The tradeoff between imperceptibility and robustness is that: if imperceptibility is increased, robustness will degrade [13].

TABLE II: PERFORMANCE COMPARISON AFTER NOISE INSERTION

Noise Density	Image	PSNR (dB)		NCC	
		DCT	FWHT-DCT	DCT	FWHT-DCT
0.5	Lena	37.1401	43.0127	0.9989	0.9971
	Boat	37.1405	42.3187	0.9849	0.9997
	Pepper	37.1401	42.1067	0.9986	0.9906
	AI ^a	5.8725		-0.0029	
1.0	Lena	36.8831	42.1108	0.9986	0.9969
	Boat	36.8834	41.3956	0.9840	0.9997
	Pepper	36.8831	41.1022	0.9983	0.9900
	AI ^a	5.2276		-0.0032	
1.5	Lena	36.5064	40.9303	0.9991	0.9971
	Boat	36.5067	39.4166	0.9840	0.9994
	Pepper	36.5064	39.1390	0.9983	0.9892
	AI ^a	4.4238		-0.0037	
2.0	Lena	36.0090	39.6816	0.9986	0.9991
	Boat	36.0093	38.5402	0.9846	0.9991
	Pepper	36.0090	38.1076	0.9986	0.9886
	AI ^a	3.6725		-0.0032	

^a AI=Average Improvement

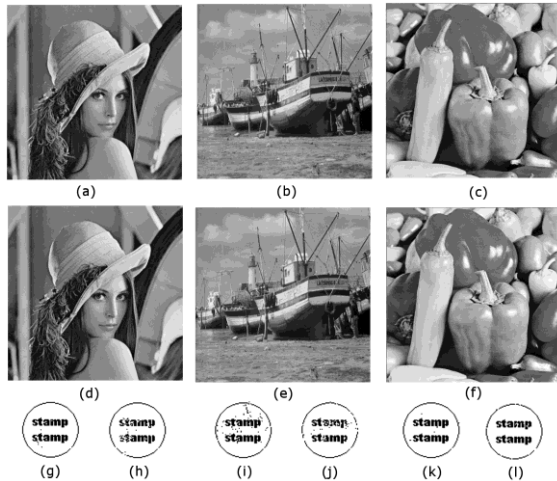


Fig. 4. Watermarked image and recovered watermark after noise insertion ($d=1.0$); (a)-(c) watermarked image with DCT, (d)-(f) watermarked image with FWHT-DCT, (g)&(h) recovered image from (a)&(d), (i)&(j) recovered image from (b)&(e), (k)&(l) recovered image from (c)&(f).

In this experiment, several values of d are used to test the imperceptibility and robustness after noise insertion. The performance comparison between FWHT-DCT and DCT scheme is shown in Table II. Fig. 4 shows the sample of the watermarked images and recovered watermarks with noise density $d=1$. The image quality (PSNR) of FWHT-DCT is significantly better than DCT and both watermarks are clearly recognizable.

2) JPEG compression attack

JPEG is commonly used for lossy compression at digital images, allowing significant reduction in size without visual loss of image quality using a variable compression factor or quality factor (Q -factor). The Q -factor is a number that determines the degree of loss in the compression process. Such a process causes the structure or format of the image to be changed, so the watermarked image would be affected.

TABLE III: PERFORMANCE COMPARISON AFTER JPEG COMPRESSION

Quality Factor (Q)	Image	PSNR (dB)		NCC	
		DCT	FWHT-DCT	DCT	FWHT-DCT
30	Lena	35.0381	38.0279	0.9989	0.9936
	Boat	34.0012	36.7351	0.9826	1.0000
	Pepper	34.4534	36.8767	0.9989	0.9616
	AI ^a	2.7157		-0.0084	
40	Lena	36.0455	39.7736	0.9989	0.9936
	Boat	35.3303	38.4511	0.9837	0.9991
	Pepper	35.4754	38.5306	0.9983	0.9741
	AI ^a	3.3014		-0.0047	
50	Lena	36.6548	41.3880	0.9989	0.9936
	Boat	36.4271	40.7360	0.9846	0.9993
	Pepper	36.2461	40.2561	0.9983	0.9741
	AI ^a	4.3507		-0.0049	
60	Lena	37.0867	42.8170	0.9989	0.9936
	Boat	37.0933	42.8425	0.9846	0.9984
	Pepper	36.9774	42.4144	0.9983	0.9741
	AI ^a	5.6388		-0.0052	

^a AI=Average Improvement

Experiments with JPEG compression is performed using several Q values. The performance comparison of the two schemes is shown in Table III. After JPEG compression, the

watermarks were recovered successfully, as shown in Fig. 5. Again, similar results were noticed.

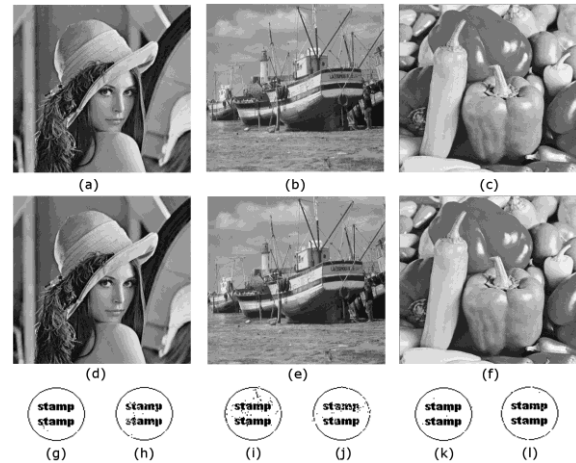


Fig. 5. Watermarked image and recovered watermark after JPEG compression ($Q=50$); (a)-(c) watermarked image with DCT, (d)-(f) watermarked image with FWHT-DCT, (g)&(h) recovered image from (a)&(d), (i)&(j) recovered image from (b)&(e), (k)&(l) recovered image from (c)&(f).

3) Image Cropping Attack

This experiment is applied by cutting the part of the watermarked image in the specific rows and columns. In this attack, part of the watermarked image is lost, thus part of watermark is also lost. Consequently, the quality of the watermarked image is degraded after this operation. When larger areas are cropped, there would be more distortion. Even with image cropping, the proposed scheme is significantly more perceptible with higher PSNR value than the DCT scheme, as shown in Table IV. Fig. 6 shows the recovered watermarks after cropped by 15% of size.

TABLE IV: PERFORMANCE COMPARISON AFTER IMAGE CROPPING

Percent of Cropping (C)	Image	PSNR (dB)		NCC	
		DCT	FWHT-DCT	DCT	FWHT-DCT
10%	Lena	16.1749	21.0259	0.9031	0.9082
	Boat	14.0038	21.1051	0.8899	0.9107
	Pepper	15.3097	21.1785	0.9031	0.9008
	AI ^a	5.9404		0.0079	
15%	Lena	14.2939	20.7897	0.8526	0.8569
	Boat	12.3990	20.7869	0.8409	0.8591
	Pepper	13.7053	20.9489	0.8523	0.8492
	AI ^a	7.3758		0.0065	
20%	Lena	12.7936	20.4952	0.8044	0.8101
	Boat	11.2003	20.4333	0.7944	0.8124
	Pepper	12.5113	20.7003	0.8044	0.8033
	AI ^a	8.3745		0.0075	
30%	Lena	11.6362	20.1643	0.7511	0.7616
	Boat	10.3764	20.2018	0.7462	0.7633
	Pepper	11.4615	20.3988	0.7522	0.7536
	AI ^a	9.0969		0.0097	

^a AI=Average Improvement

4) Image Rotation Attack

This experiment is performed by applying a degree of rotation on the watermarked image. As a square matrix, rotation produces a larger image than the original. As such, the resulting image from the rotation is cropped to fit the size

of the watermark. Using several rotation angles, the proposed scheme was found to be significantly better, at most angles of rotation than the DCT scheme.

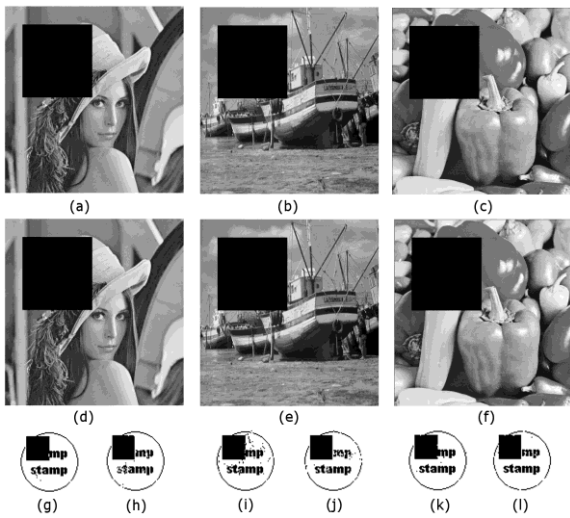


Fig. 6. Watermarked image and recovered watermark after cropping($C=15\%$); (a)-(c) watermarked image with DCT, (d)-(f) watermarked image with FWHT-DCT, (g)&(h) recovered image from (a)&(d), (i)&(j) recovered image from (b)&(e), (k)&(l) recovered image from (c)&(f).

TABLE V: PERFORMANCE COMPARISON AFTER IMAGE ROTATION

Rotation Angle (θ)	Image	PSNR (dB)		NCC	
		DCT	FWHT-DCT	DCT	FWHT-DCT
45°	Lena	6.4181	20.7103	0.4120	0.8915
	Boat	6.2690	20.8579	0.4109	0.8955
	Pepper	6.4945	20.6328	0.4063	0.8825
	AI ^a	14.3398		0.4801	
90°	Lena	6.4145	21.4324	0.1049	0.8475
	Boat	6.2654	21.7555	0.1785	0.8458
	Pepper	6.4898	21.6471	0.1283	0.8509
	AI ^a	15.2218		0.7108	
135°	Lena	6.4247	20.7121	0.4052	0.8834
	Boat	6.2801	20.8619	0.4103	0.8861
	Pepper	6.4998	20.6398	0.4052	0.8834
	AI ^a	14.3364		0.4774	
180°	Lena	6.4248	21.4367	0.0969	0.7455
	Boat	6.2804	21.7550	0.1081	0.7733
	Pepper	6.5000	21.6441	0.0978	0.7587
	AI ^a	15.2102		0.6582	

^a AI=Average Improvement

The comparison of the two schemes is shown in Table V, and the recovered watermarks are shown in Fig. 7. The strength of the proposed technique is obvious in this attack, where there is very significant improvement of quality in both the watermarked image (visually similar but large difference

in PSNR values) and watermark. The watermark in the DCT is unrecognizable in this type of attack.

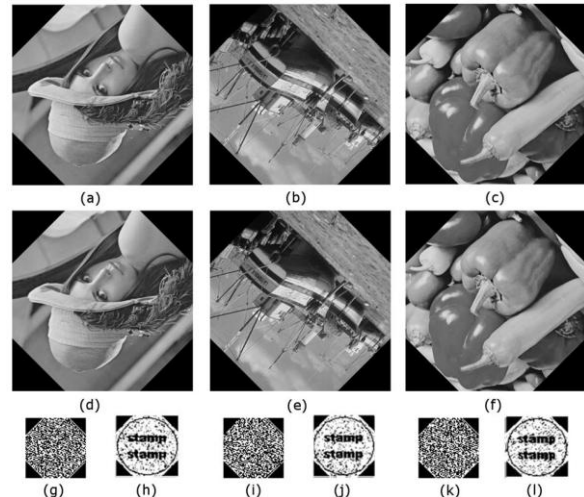


Fig. 7. Watermarked image and recovered watermark after image rotation ($\theta=135^\circ$); (a)-(c) watermarked image with DCT, (d)-(f) watermarked image with FWHT-DCT, (g)&(h) recovered image from (a)&(d), (i)&(j) recovered image from (b)&(e), (k)&(l) recovered image from (c)&(f).

5) Image Resizing Attack

This experiment is performed by applying a scaling factor for image resizing, i.e. shrinking and dilation. The change in size tampers with both the watermarked image and watermark. The results of this experiment using various resizing scales are shown in Table VI. Enlarging the watermarked image produced high perceptual invisibility.

TABLE VI: PERFORMANCE COMPARISON AFTER IMAGE RESIZING

Scaling Factor (x)	Image	PSNR (dB)		NCC	
		DCT	FWHT-DCT	DCT	FWHT-DCT
0.4 [325x325]	Lena	5.6965	14.6419	0.4924	0.8235
	Boat	5.3907	14.9806	0.4833	0.8460
	Pepper	5.4901	14.9703	0.4882	0.8529
	AI ^a	9.3385		0.3528	
0.5 [256x512]	Lena	5.6942	13.6175	0.4645	0.8489
	Boat	5.3831	13.9684	0.4762	0.8358
	Pepper	5.4889	13.9568	0.4902	0.8611
	AI ^a	8.3255		0.3716	
0.5 [512x256]	Lena	5.6978	16.6306	0.4862	0.8281
	Boat	5.3937	16.9657	0.4936	0.8628
	Pepper	5.4894	16.9732	0.4887	0.8797
	AI ^a	11.3295		0.3674	
1.5 [628x628]	Lena	5.6923	17.5335	0.4870	0.8486
	Boat	5.3814	17.8889	0.4865	0.8494
	Pepper	5.4859	17.8701	0.4950	0.8611
	AI ^a	12.2443		0.3635	

^a AI=Average Improvement

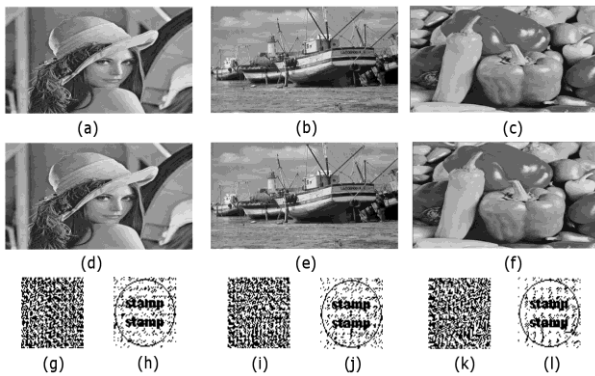


Fig. 8. Watermarked image and recovered watermark after image resizing (0.5x); (a)-(c) watermarked image with DCT, (d)-(f) watermarked image with FWHT-DCT, (g)&(h) recovered image from (a)&(d), (i)&(j) recovered image from (b)&(e), (k)&(l) recovered image from (c)&(f).

Furthermore, Fig. 8 shows the watermark which recovered by the proposed scheme. The watermark has a noise but still identifiable. As with the previous experiment, the proposed technique's resilience is apparent in this attack as compared to the unrecognizable watermark result in the DCT approach.

VI. CONCLUSION

This paper has proposed an improved more resilience watermarking scheme. Evaluation of the watermarking performance of the proposed scheme was undertaken against the DCT scheme. In all the test cases, transforming the watermark using the FWHT-DCT improved the imperceptibility of the watermarked image. The proposed scheme is also proven to have good robustness against attacks, significantly so when the images are rotated or resized. As a future work, the Fast Walsh Hadamard transform will be implemented on the other common domains, such as SVD and DWT to evaluate its performance in order to improve a performance of watermarking scheme.

REFERENCES

- [1] I. J. Cox, M. L. Miller, and J. A. Bloom, "Watermarking applications and their properties," in *Proc. of the International Conference on Information Technology: Coding and Computing (ITCC 2000)*, Las Vegas, NV, USA, 27-29 March, 2000, pp. 6-10.
- [2] M. Sharkas, D. El-Shafie, and N. Hamdy, "A dual digital-image watermarking technique," in *Proc. of the World Academy of Science, Engineering and Technology*, vol. 5, 2005, pp. 136-139.
- [3] V. M. Potdar, S. Han, and E. Chang, "A survey of digital image watermarking techniques," in *Proc. of the 3rd IEEE Inter. Con. on Industrial Informatics (INDIN '05)*, 2005, pp. 709-716.
- [4] M. E. G. Mona, "Comparison between two watermarking algorithms using DCT coefficient and LSB replacement," *Journal of Theoretical and Applied Information Technology*, vol. 4, no. 2, 2008, pp. 132-131.
- [5] Z. Daxing, X. Junfeng, L. Haihua, and L. Heming, "A novel image watermarking algorithm with fast processing speed," in *Proc. of the International Conference on Information Engineering and Computer Science*, 2009, pp. 1-4.
- [6] A. Al-Haj, "Combined DWT-DCT digital image watermarking," *Journal of Computer Science*, vol. 3, no. 9, 2007, pp. 740-746.
- [7] G. Bhatnagar and B. Raman, "Robust watermarking in multiresolution walsh-hadamard transform," in *Proc. of the IEEE International Advance Computing Conference*, India, 2009, pp. 894-899.
- [8] H. Li, S. Wang, W. Song, and Q. Wen, "Multiple watermarking using hadamard transform," *Lecture Notes in Computer Science (LNCS)*, vol. 3739, 2005, pp. 767-772.

- [9] S. Saryadzi and H. Nezamabadi-pour, "A blind digital watermark in hadamard domain," in *Proc. of the World Academy of Science, Engineering and Technology*, vol. 3, 2005, pp. 245-248.
- [10] A. aung, P. N. Boon, and S. Rahardja, "A robust watermarking scheme using sequency-ordered complex Hadamard transform," in *Journal of Signal Processing System*, vol. 64, no. 3, 2010, pp. 319-333.
- [11] R. Kountchev, S. Rubin, M. Milanova, V. Todorov, and R. Kountcheva, "Resistant image watermarking in the phases of the complex hadamard transform coefficients," in *Proc. of the IEEE International Conference on Information Reuse and Integration*, 2010, pp. 159-164.
- [12] S. P. Maitya and M. K. Kundub, "Perceptually adaptive spread transform image watermarking scheme using hadamard transform," *Journal of Information Sciences*, vol. 181, no. 3, 2011, pp. 450-465.
- [13] A. Marjuni, R. Logeswaran, and M. F. Ahmad Fauzi, "An image watermarking scheme based on fast walsh hadamard transformation and discrete cosine transformation," in *Proc. of International Conference on Networking and Information Technology*, pp. 289-293, June 2010.
- [14] A. K. Jain, *Fundamentals of Digital Image Processing*, Prentice-Hall International, Singapore, 1989, Ch. 5, pp. 155-159.
- [15] W. K. Pratt, *Digital Image Processing*, Wiley-Interscience, John Wiley & Sons, New Jersey, 2007, pp. 204-210.
- [16] D. Sundararajan, *The Discrete Fourier Transform: Theory, Algorithms and Applications*, World Scientific Publishing, Singapore, 2001, Ch. 15-16, pp. 303-329.
- [17] R. Moore and N. Drakos. Walsh-Hadamard Transform. Mathematics Department. Macquarie University. Sydney. 1999. [Online]. Available : <http://fourier.eng.hmc.edu/e161/lectures/wht/wht.html>.



image processing.

Aris Marjuni graduated with a Bachelor degree in Mathematics from Diponegoro University, Semarang, Indonesia in 1993, and a Master of Informatics Engineering degree from STTI Benarief, Jakarta, Indonesia in 2001. He is currently studying at Faculty of Engineering, Multimedia University, Cyberjaya, Malaysia. His present research interest is in the area of



information processing.

Mohammad Faizal Ahmad Fauzi received the B.Eng. degree in electrical and electronic engineering from Imperial College, London, UK in 1999, and the Ph.D. degree in electronics and computer science from University of Southampton, Southampton, UK in 2004. He is currently attached to the Multimedia University, Malaysia as a lecturer/researcher. His main research interests are in the area of signal processing, analysis, retrieval and compression of image, audio and video data, as well as biometrics.



information processing.

Rajasvaran Logeswaran received his B. Eng. (Hons) Computing degree from the University of London (Imperial College of Science, Technology and Medicine), United Kingdom in 1997, M.Eng.Sc. and Ph.D. degrees from Multimedia University, Cyberjaya in 2000 and 2006, respectively. He was an Assistant Professor at The Global School of Media, Soongsil University, South Korea in 2008. He is currently an Associates Professor at School of Engineering, Science and Technology, Nilai University College, Nilai, Negeri Sembilan, Malaysia. His research interests comprises of neural network, data compression, medical image processing and web technology.



information security.

Swee-Huay Heng received her B.Sc. (Hons) and M.Sc degrees from University Putra Malaysia (UPM), and her Doctor of Engineering degree from the Tokyo Institute of Technology, Japan. She is currently a lecturer in the Faculty of Information Science & Technology, Multimedia University, Malaysia. Her research interests include cryptography and